tvst

https://doi.org/10.1167/tvst.8.6.39

Article

Confocal and Histological Features After Poly(Ethylene Glycol) Diacrylate Corneal Inlay Implantation

Aritz Bidaguren[1], Javier Mendicute[1], Iratxe Madarieta[2], and Nerea Garagorri[2]

[1] Donostia University Hospital, San Sebastian, Spain
[2] Tecnalia Research and Innovation, San Sebastian, Spain

Correspondence: Aritz Bidaguren, Paseo Doctor Begiristain 109, San Sebastian 20014, Spain. e-mail: aritzbidaguren@gmail.com

Received: 14 February 2019
Accepted: 24 October 2019
Published: 18 December 2019

Keywords: poly(ethylene glycol) diacrylate; confocal microscopy; hydrogel; intracorneal inlay; corneal stroma

Citation: Bidaguren A, Mendicute J, Madarieta I, Garagorri N. Confocal and histological features after poly(ethylene glycol) diacrylate corneal inlay implantation. Trans Vis Sci Tech. 2019;8(6):39, https://doi.org/10.1167/tvst.8.6.39

Purpose: To evaluate the in vivo biocompatibility of photopolymerized poly(ethylene glycol) diacrylate (PEGDA) intrastromal inlays in rabbit corneas.

Methods: Sixty-three eyes of 42 New Zealand rabbits were included. Manual intrastromal pockets were dissected in 42 eyes. PEGDA inlays were obtained using a specifically designed photomask and were inserted in the intrastromal pocket of 21 eyes (inlay group); the remaining 21 right eyes did not receive any implant (pocket-only group). Twenty-one eyes with no intervention were used as controls. In vivo confocal microscopy (IVCM) was performed at every visit. After 2 months, rabbits were sacrificed and corneas removed for histological analysis.

Results: Corneas remained clear in all but two animals, and five cases of corneal neovascularization were seen ($P = 0.2$). Inlays remained stable without evidence of lateral or anterior migration, and no other complications were observed. No changes in anterior and posterior keratocyte density ($P = 0.3$ and $P = 0.1$, respectively) or endothelial cell density ($P = 0.23$) were observed between groups during the study time by IVCM. On pathology samples, thinning of the epithelium over the inlay area and epithelial hyperplasia over the edges were observed. A polygonal empty space with no evidence of PEGDA hydrogel within the midstroma was seen in the inlay group. Keratocytes were normal in shape and number in the vicinity of the PEGDA implant area.

Conclusions: Photopolymerized PEGDA intrastromal inlays have shown relatively good safety and stability in rabbit corneas. Inlays were biostable in the corneal environment and remained transparent during follow up.

Translational Relevance: The investigated PEGDA is promising for the development of biocompatible intrastromal implants.

Introduction

There are several methods to correct refractive errors, namely, ablative (laser-based), incisional, or additive techniques, including intrastromal segments and intrastromal inlay implantations. Intracorneal inlay implantation for the correction of ametropias is a technique known as keratophakia, and it was described by JI Barraquer in 1949.[1] Since Barraquer's first attempts to modify corneal shape by means of intrastromal inlay implantations, implants made of human corneas (homoplastic implants) and synthetic materials (haloplastic implants) have been developed and implanted in human and animal corneas with variable results.[2–4]

Initial attempts were made with high refractive index (RI)-impermeable materials, such as polysulfone and polymethylmethacrylate (PMMA), aiming to modify refractive errors by increasing the RI of the cornea.[1,5–12] Complications such as epithelial thinning, corneal opacity, stromal necrosis, and implant extrusion were observed and attributed to the lack of permeability of the material, evidencing the absolute requirement for water and glucose permeability of the inlays.[13,14] After initial complications with impermeable materials, high water content and high permeability hydrogels were developed and implanted into

corneas, with the objective of modifying corneal curvature.

Optical properties and permeability of hydrogels have been known since the early 1960s, but it was not until 1967 that Dohlman first used hydrogel material as an intrastromal inlay.[15] Since then, several articles have documented the biocompatibility of different hydrogel inlays in humans and animals in the long term.[16–29] More recently, there has been emerging interest in corneal inlays as potential methods for the correction of presbyopia, and implants made of different materials and designs have been developed for this purpose.[30–42]

Hydrogels are crosslinked hydrophilic polymers with properties that mimic those of the natural cornea. Besides the refractive purpose described previously, they have also been used for tissue replacement as artificial corneas in research studies,[43–46] and there is a commercialized hydrogel-based keratoprostheses (AlphaCor).[47] Photopolymerized hydrogels have been investigated in vitro for tissue engineering and microsphere and keratocyte encapsulation.[48–50] These features, together with the optical clarity, water content, swelling behavior, and flexibility shown by photopolymerized hydrogels, make them suitable for ophthalmic applications.[44,46]

The aim of this study was to assess the in vivo biocompatibility of a poly(ethylene glycol) diacrylate (PEGDA) hydrogel. PEGDA inlays were photopolymerized and implanted intralamellarly into rabbit corneas. Biomicroscopy and in vivo confocal microscopy (IVCM) analysis were performed, and rabbits were sacrificed and corneas removed for histological assessment after 2 months. Cellular changes were analyzed by IVCM at different corneal depths, and results were later compared with histological samples.

Materials and Methods

A prospective interventional study including 63 eyes of 42 female New Zealand rabbits weighting between 2.8 and 3.6 kg was conducted. Eyes were divided in three groups. Group 1 (pocket-only group) included 21 right eyes with intrastromal pocket and no inlay implantation. Group 2 (inlay group) included 21 right eyes with a PEGDA hydrogel corneal intrastromal inlay implant after a lamellar stromal pocket dissection. (Fig. 1) Twenty-one left eyes of rabbits of group 1 with no intervention were used as controls (control group). All animals were treated in accordance with the guidelines of the Association for Research in Vision and Ophthalmology for the Use and Care of Animals in Research.

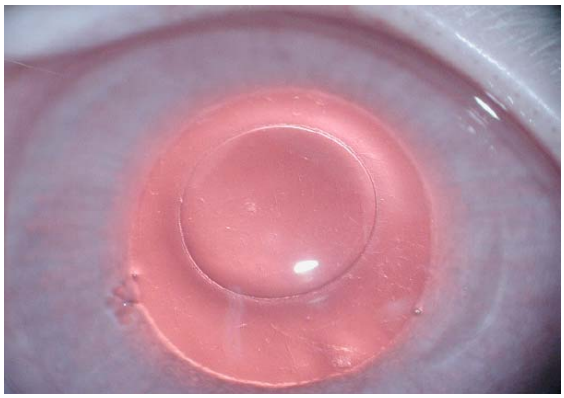

Figure 1. Biomicroscopy of PEGDA intracorneal inlay in the rabbit eye.

Intracorneal Inlays

Inlays were designed and developed at the Health Division-Biomaterials area of Tecnalia Research and Innovation (Spain). Hydrogel inlays were formed by photopolymerization of a 30% w/v concentration of 3400 Da molecular weight PEGDA (Nektar, Hundsville, AL). The photoinitiator used in the photopolymerization process was Irgacure 2959 (5%).

The photopolymerization process was performed according to previously determined procedures.[47] Briefly, PEGDA was dissolved in phosphate-buffered saline (pH 7.4) to form 10% (w/v) solutions. The 2-hydroxy-1-[4-(hydroxyethoxy)phenyl]-2-methyl-1-propanone photoinitiator (Irgacure 2959; Ciba Specialty Chemicals, Basel, Switzerland) was used dissolved in a 70:30 ethanol:water mixture and added to the polymer solution at a final concentration of 0.05% (w/w) with respect to the PEGDA. Photopolymerization of the macromere was carried out using a 365-nm UV light (Fisher Scientific, Madrid, Spain) at a 4-mW/cm^2 intensity for 5 minutes.

PEGDA was cast into inlays by using photomask molds specifically designed for this purpose to obtain 4-mm-diameter and 100-µm-thickness inlays. Resulted inlays were washed in Milli-Q water and immediately transported in specific recipients for the implantation.

Surgery

Surgeries were performed under a surgical microscope (Leica M651; Leica Microsystems, Heerbrugg, Switzerland) by the same experienced surgeon. Rabbits were anesthetized with a combination of 35

mg/kg intramuscular ketamine hydrochloride and 5 mg/kg xylazine hydrochloride and topical tetracaine and oxybuprocaine drops. After ultrasound pachymetry measurement, 5-mm-length and 250-μm-depth incisions were performed with a calibrated diamond blade, and manual lamellar pockets were dissected with Melles dissectors (DORC, Zuidland, Netherlands). Stromal pockets were then irrigated with filtered balance salt solution to remove possible debris. Intrastromal corneal inlays were centered inside the stromal pocket and incisions sutured with 10-0 nylon (Alcon Surgical, Fort Worth, TX). Sutures were removed 1 week after surgery. In corneas of group 1, an identical procedure was followed but no inlay was implanted.

Follow-Up

All rabbits were subjected to routine slit lamp postoperatory examinations at 1, 7, 15, 30, and 60 days after surgery. Postoperatively, eyes were treated with tobramycin eye drops (Tobrex) every 6 hours for 1 week. Every examination included an assessment of the conjunctiva, corneal transparency anterior and posterior to the inlay, epithelial integrity, intracorneal inlay position, and inlay transparency.

Confocal Microscopy

IVCM was performed in all corneas preoperatively and at postoperative days 7, 30, and 60, in groups 1 and 2 by the same examiner. Examinations were performed using a scanning slit confocal microscope (Confoscan 4; Nidek Technologies, Padova, Italy) with a Z-ring adaptor to ensure uniform pressure at the cornea throughout the scan. Examinations were performed under the same topical and intramuscular anesthesia described previously. A drop of methylcellulose solution was placed on the tip of the 40× immersion objective lens (Zeiss, Oberkochen, Germany), and corneas were aligned to scan the central cornea. Two to three full-thickness automatic corneal scans were performed in every examination, and 350 images were recorded. Scans with inadequate image quality were excluded from the quantitative analysis.

Anterior and posterior stromal keratocyte density were manually calculated as the mean cell number within a 200-μm^2 area of two to three different images at each depth, and results were given as cells per square millimeter. Qualitative and quantitative central corneal endothelial analyses were performed by the semiautomatic image analyzing system of the NAVIS software provided by the Confoscan 4 microscope. Mean endothelial cell density, mean endothelial cell area, coefficient of variation of endothelial cell area, and the percentage of hexagonal cells were studied. Evaluation of IVCM images was done in a masked fashion by the same examiner.

Histology

Rabbits were sacrificed after final exploration at 2 months, and corneas were removed for histological assessment. Corneas were fixed in a 4% paraformaldehyde solution for 24 hours, and paraffin blocks were made. Sections of 5 μm were cut limbus to limbus onto slides and stained with hematoxylin-eosin following routine procedures.

Statistics

Software-based statistical analysis was performed (SPSS; SPSS Sciences 19.0, Chicago, IL). Normality of variables was analyzed with the Kolmogorov-Smirnov test. The χ^2 test was used for categorical variables. Parametric tests used were Student's *t*-test and paired Student's *t*-test for intragroup mean comparison. The general linear model (GLM) repeated measures procedure was used to analyze mean differences between groups at different time points. The level of statistical significance was $P < 0.05$.

Results

PEGDA Implants

The water content of the inlays was 79%, the volumetric swollen ratio (Q) was 0.78 ± 0.15 and their glucose diffusion coefficient (D) was $1.11 \times 10^{-9} \pm 0.10 \times 10^{-9}$ (cm^2/s). The glucose diffusion coefficient (D) of the ex vivo corneas used as reference was $1.87 \times 10^{-9} \pm 0.32 \times 10^{-9}$ (cm^2/s). The inlays had a 4 mm diameter, central thickness of 100 μm, and RI of 1.35.

Clinical Examination

The surgical procedure was completed in 42 right eyes (21 of group 1 and 21 of group 2), and all animals remained in the study until the predetermined final time point. The control group consisted of 21 left eyes that had no surgical intervention. No intraoperative complications occurred in any of the groups. Corneas remained biomicroscopically clear at day 60 in all cases except in two eyes (one in group 1 and one in group 2). The epithelium remained intact, and no epithelial defects, corneal

Table 1. Keratocyte Density by IVCM

	Preoperative		Day 7	
Parameter	Group 1	Group 2	Group 1	Group 2
AKD, cells/mm^2, mean ± SD	1035 ± 98	1010 ± 97	1095 ± 196	1040 ± 101
PKD, cells/mm^2, mean ± SD	702 ± 92	670 ± 99	803 ± 110	658 ± 139

AKD, anterior keratocyte density; PKD, posterior keratocyte density.

Table 1. Extended

	Day 30		Day 60		
Parameter	Group 1	Group 2	Group 1	Group 2	*P* Value
AKD, cells/mm^2, mean ± SD	1034 ± 187	1002 ± 177	1111 ± 159	934 ± 325	0.33
PKD, cells/mm^2, mean ± SD	735 ± 105	779 ± 123	665 ± 123	665 ± 140	0.1

ulcers, or epithelial ingrowths were observed during follow-up. Mild conjunctival injection was observed in 35% and 33% of cases (groups 1 and 2, respectively) in postoperative day 7. All of them resolved favorably by postoperative day 60. Stromal edema was seen in 40% and 11% of cases of group 1 and 43% and 33% of cases of group 2 at postoperative days 1 and 7, respectively. All cases of edema underwent complete resolution by day 60 except two (one case in group 1 and one case in group 2). These two cases associated corneal infiltration and were the only cases with corneal opacity at day 60. No other cases of significant clinical haze were seen at final exploration in the inlay group. There were five cases of corneal superficial neovascularization (one case in group 1 and four cases in group 2), with no statistically significant differences between groups ($P = 0.2$). No cases of stromal thinning or melting were observed. Inlays remained optically clear during follow-up in all cases, including the case with the stromal infiltration, and their position remained stable with no evidence of lateral or anterior migration of the inlays throughout the study.

In Vivo Confocal Microscopy

Two major peaks of reflectivity, corresponding to the endothelium and the superficial epithelium and a minor peak in the midstroma corresponding to the interface, were observed on the z-scan graphic of corneas in group 1. Z-scan graphics of corneas in group 2 showed similar epithelial and endothelial reflectivity peaks and a depression of the reflectivity in the midstromal area, corresponding to the inlay.

Superficial, intermediate, and basal cell layers of the epithelium were observed by IVCM in all cases, with no morphologic differences between groups. There was no evidence of abnormal structures on the epithelium in any of the groups analyzed. Activated keratocytes in the anterior stroma (anterior to the inlay) were seen in all cases at postoperative days 7, 30, and 60. No keratocyte activation was seen below the lamellar dissection. Mean anterior and posterior keratocyte density values in every examination are shown in Table 1. Anterior and posterior keratocyte density did not show statistically significant differences inside group 1 (anterior stroma, $P = 0.23$; posterior stroma, $P = 0.11$) or group 2 (anterior stroma, $P = 0.76$; posterior stroma, $P = 0.27$) during the follow-up period. There was no statistically significant change in the anterior ($P = 0.33$) or posterior ($P = 0.1$) keratocyte cell density between groups 1 and 2 during follow-up (GLM repeated measures procedure). Endothelial cell density, endothelial cell area, percentage of hexagonal cells, and coefficient of variation of cell area values recorded during follow-up are shown in Table 2. No endothelial cell loss was seen in group 1 ($P = 0.07$) or group 2 ($P = 0.23$) during postoperative follow-up. There was no statistically significant change in the endothelial cell density, endothelial cell area, percentage of hexagonal cells, or in the coefficient of variation of cell area between groups during follow-up (GLM repeated measures procedure).

Histology

Corneas with no intervention (control group) showed normal tissue properties, such as regularly

Table 2. Endothelial Cell Features Measured by IVCM

	Preoperative		Day 7	
Parameter	Group 1	Group 2	Group 1	Group 2
ECD, cells/mm^2, mean ± SD	2879 ± 310	2874 ± 280	2844 ± 307	3153 ± 240
MCA, mm^2, mean ± SD	351 ± 38	344 ± 38	354 ± 37	318 ± 23
CVCA, mean ± SD	19 ± 6.5	17 ± 6	22,23 ± 9.3	30.65 ± 11.2
HEC, %, mean ± SD	66 ± 6	67 ± 6	63 ± 8	50 ± 14

ECD, endothelial cell density; MCA, mean cell area; CVCA, coefficient of variation of cell area; HEC, hexagonal endothelial cells.

Table 2. Extended

	Day 30		Day 60		
Parameter	Group 1	Group 2	Group 1	Group 2	*P* Value
ECD, cells/mm^2, mean ± SD	2720 ± 288	2974 ± 248	2739 ± 201	2957 ± 293	0.23
MCA, mm^2, mean ± SD	371 ± 40	338 ± 28	367 ± 28	34 ± 34	0.26
CVCA, mean ± SD	19.04 ± 6.5	21.22 ± 8	16.7 ± 5.9	24.6 ± 7.1	0.2
HEC, %, mean ± SD	59 ± 9	60 ± 9	66 ± 10	64 ± 5	0.26

spaced collagen fibers with keratocytes embedded in the stroma, stratified epithelium, a monolayer of plane endothelial cells, and no evidence of inflammatory cells. Corneas of group 1 (pocket-only) showed similar features to untouched control corneas. The epithelium remained unaltered, and the epithelial thinning was only observed in one case. There was no histologic evidence of corneal interface except for four cases (Fig. 2). Three of these cases had clear corneas on biomicroscopy and the fourth corresponded to the case with stromal infiltration and associated eosinophilic inflammatory infiltration. Corneas of group 2 (inlay group) (Fig. 3) showed thinning of the stratified epithelium above the inlay and epithelial hyperplasia over the edges of the inlay. A polygonal empty space within the midstroma, where the PEGDA inlay was implanted, was observed in all cases. PEGDA hydrogel inlays were not visible in contact with the surrounding stroma in their original place and shape, and small, distorted hydrogel fragments were occasionally observed. There was a compression of collagen lamellas on the edge of the inlays, with no evidence of fibrous capsule formation around the pocket. Keratocyte nuclei were visible at the edges of the polygonal empty space, and inflammatory eosinophilic stromal infiltration was observed in one case. This case showed clinical stromal infiltration on biomicroscopy.

Discussion

The purpose of this study was to evaluate the biocompatibility of photopolymerized PEGDA inlays after intrastromal implantation in rabbit corneas to be used with therapeutic purpose as a keratoprosthesis. Clinical results were then compared with IVCM findings and with histology samples of the corneas. To investigate the biocompatibility of PEGDA implants with corneal stroma, corneas with inlays were compared with a group of corneas with stromal pockets and no implant and with control corneas over a 2-month period.

Hydrogel inlays made of different materials and designs have shown efficacy and safety after intrastromal implantation in human and rabbit corneas.[22,39,44,46,51–54] Poly(ethylene glycol) (PEG) is a biocompatible polymer used extensively as biomaterial in medicine,[43] and it has shown good biocompatibility when used as intrastromal inlay.[44,52,53] PEG is soluble in aqueous solutions and can be easily modified on exposure to UV light to form cross-linked hydrogels of high water content.[52] Water content, optical properties, and mechanical stability make PEG-based implants suitable to be used as artificial corneas.[55] PEGDA macromere-based photopolymerized hydrogels have also been tested in vitro for keratocyte encapsulation and drug delivery vehicles.[56] These properties of PEGDA-based photo-

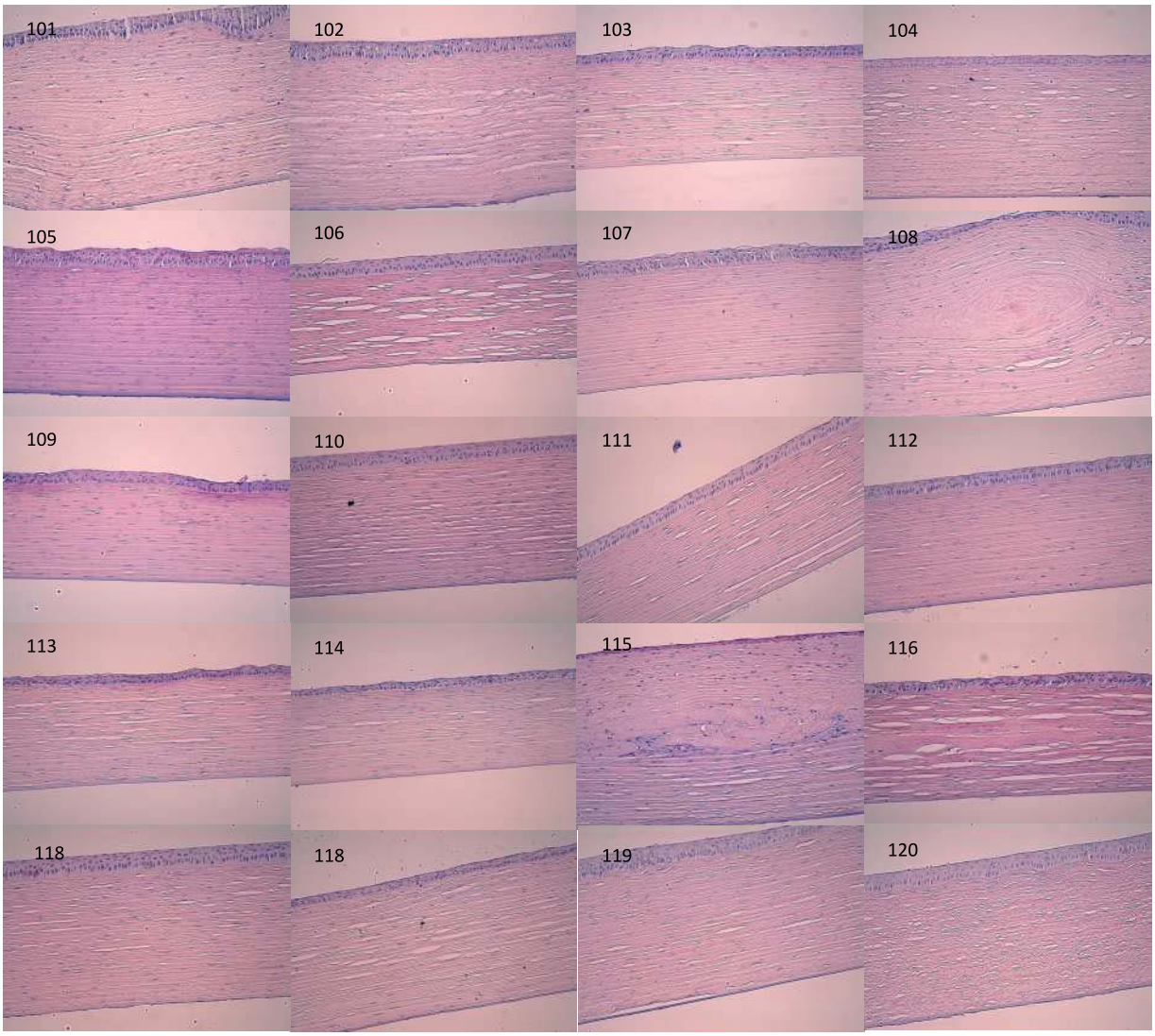

Figure 2. Pathology samples of corneal tissues of rabbits in group 1 (pocket-only). Hematoxylin-eosin staining. Normal endothelium, stroma, and epithelium are observed in all cases except for four cases. These four cases (identifiers 101, 108, 115, and 116) showed midstromal fibrosis with irregularities of the collagen organization and absence of keratocytes around the scarring tissue.

polymerized hydrogels make them potentially suitable for corneal tissue engineering and the development of skirts for keratoprosthesis.

In vivo biocompatibility of stromal inlays depends on different factors such as the surgical procedure, the animal species, postoperative conditions, and especially glucose and water permeability of the material.[13,15,54] Glucose diffusion coefficient of the photopolymerized 30% PEGDA inlay was analyzed in vitro, and results were compared with the glucose diffusion coefficient of ex vivo rabbit corneas, showing equivalent permeability. An absence of melting, thinning of the cornea or ulceration, as well as histologic results corroborate well with the in vivo permeability of the 30% (w/v) PEGDA inlays. IVCM images and histology samples showing healthy epithelium and stroma corroborate clinical biocompatibility. Comparative clinical data from control, sham-operated, and implanted corneas showed little response to the presence of a stromal pocket and to the PEGDA intrastromal inlay, with no statistically significant differences observed between groups with or without inlay in any of the clinical variables analyzed. Optical properties of the PEGDA inlays did not change during the study and implants remained optically clear and stable, with no cases of migration observed during follow-up.

Several complications, such as corneal neovascu-

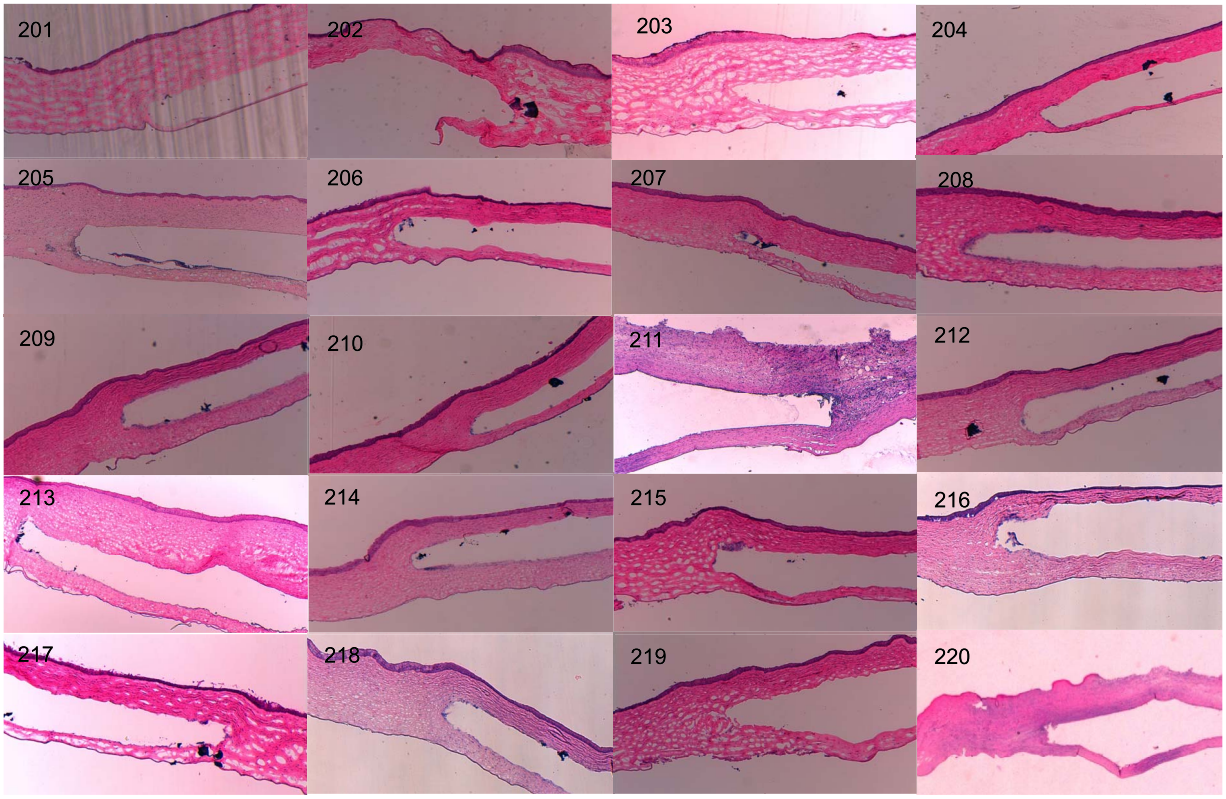

Figure 3. Corneal tissues of rabbits in group 2 (inlay). Hematoxylin-eosin staining. Optically clear polygonal empty spaces are observed in all cases with no evidence of PEGDA hydrogel inlays. Compression of collagen lamellas on the edge of the pockets and epithelial hyperplasia are visible around the empty space.

larization, haze, scarring, corneal opacity, epithelial ingrowth, inlay encapsulation, inlay decentration, and significant visual loss, in humans have been described in eyes after hydrogel permeable intrastromal inlay implantations.[22–24,27,44,54] Complications in this study were few with no statistically significant differences observed between groups with or without inlay and could not be directly attributed to the PEGDA inlay implantation. There was a maximum peak of corneal edema incidence 1 week after surgery, and the incidence decreased progressively in the following weeks in all operated eyes (sham and inlay). Only two intervened cases (one sham and one inlay) showed edema after 2 months. Similar patterns of corneal edema incidence have been described in the early phase after intrastromal implants by other authors and have been attributed to the surgical procedure rather than to the inlay implantation.[55,57] These two cases with more severe corneal edema and corneal infiltration were the only two cases with severe inflammation and corneal opacity at final exploration. The presence of severe edema with hydrogel inlays made of different materials leading to stromal infiltration and neovascularization has also been previously described.[22,58] Although most cases of corneal neovascularization after intrastromal inlay implantations described in the literature were secondary to the impermeability of the materials,[8–11] corneal neovascularization secondary to permeable hydrogel implants has also been reported, suggesting other possible causes apart from the permeability of the hydrogel.[21,57,58] Experimental models of corneal neovascularization have shown the ability of topical steroids to suppress the proliferation of stromal blood vessels in the rabbit cornea,[59,60] and it has been described that long-term use of postoperative medroxyprogesterone eye drops lead to fewer corneal melts with AlphaCor implants in humans.[61] Corneal neovascularization was observed in five cases (one sham and four inlay). Although a 20% incidence of corneal neovascularization is not to be dismissed, no statistically significant differences were observed between operated groups for the calculated sample size. Steroids were not used to control inflammatory response in this study, as evaluation of inflammatory response to PEGDA inlays was intended. However,

inflammation control is crucial to reduce complications associated with hydrogel intrastromal inlays, and the use of topical steroids could have prevented some of the complications observed.[44]

Confocal Microscopy

IVCM was used to evaluate corneal structure, morphologic features, and keratocyte and endothelial cell density after photopolymerized PEGDA intrastromal inlay implantation. Results showed little response of the corneal tissue to the presence of stromal pocket and PEGDA inlay, and this response was confined to the vicinity of the pocket and the implant. The epithelium maintained its integrity with minimal alteration of the epithelial layers in all cases (sham and inlay) over the 2-month period.

Activated keratocytes characterized by greater corneal backscattering than quiescent keratocytes, indicating a wound repair process, were observed in the anterior stroma of both groups. Although some authors report no cellular activation or corneal fibrosis by IVCM examination after intrastromal inlays of different designs and materials in rabbit corneas,[22,55] other studies have reported keratocyte activation in rabbit corneas after stromal dissection in deep anterior lamellar keratoplasty (DALK)[62] and laser-assisted in situ keratomileusis (LASIK)[63] and after hydrogel inlay insertion in humans.[24,25,64] Keratocytes posterior to the interface area appeared quiescent in every postoperative examination in our study, similar to previous reports with other intrastromal implants described in the literature.[24,39,65]

No changes in anterior and posterior keratocyte density were observed in any of the groups or between groups during follow-up. Previous studies have reported similar results, with no keratocyte density changes after lamellar dissections with microkeratome or manually dissected pockets and after different stromal inlay implants in rabbit corneas.[54,55,65] However, a decrease in keratocyte density after lamellar flaps for LASIK[66–69] and after intrastromal inlays have also been described.[64] Different studies have reported results after intrastromal inlay implantations by IVCM,[22,24,36,39,54,55,64] but comparisons of keratocyte density between surgically dissected pockets and hydrogel inlays inside the stromal pockets have not been fully analyzed. Salamatrad et al.[55] did not observe differences in keratocyte density between groups after hexafilcon hydrogel intracorneal inlays and stromal pockets by IVCM in 18 rabbit corneas 3 months after surgery, and Tan et al.[54] mention similar keratocyte density values between control, sham-operated, and implanted corneas, although density values and statistics are not mentioned. Petroll et al.[64] compared IVCM features of patients with LASIK and patients with PermaVision intracorneal lens (ICL) after corneal flaps were created with a femtosecond laser. Patients with ICL did not receive photoablation, so differences between groups could be compared between LASIK and ICL implants, but we are unaware of the differences that could be exclusively attributed to the corneal flap or the implant. To our knowledge, this is the first report of keratocyte density values after PEGDA intrastromal inlay implantation in rabbit corneas.

We did not find significant qualitative or quantitative changes in corneal endothelial cells between groups during the follow-up, and PEGDA inlay implantation did not seem to affect normal endothelial features. Similar results with an absence of endothelial cell density changes have been previously reported after LASIK and after hydrogel intrastromal inlay implantation in rabbits and in humans.[22,24,55,67,70] However, an endothelial cell density reduction has also been described after long-term follow-up with a lidofilcon A inlay in a human cornea.[29] To our knowledge, results regarding qualitative features (polymorphism and polymegethism) of the endothelium after intrastromal hydrogel inlays in rabbit corneas have not been previously reported.

Histology

Although described previously after lamellar surgery, no thinning of the epithelium was observed in corneas of group 1 (pocket-only) on histological analysis. The reasons for epithelial thinning after lamellar dissection are not fully understood, and different causes, including cutting the corneal nerves[71,72] and the particularity of the species (rabbit),[52,73] have been suggested as a possible cause. Epithelial thinning over the inlay area, as observed in the corneas of group 2, has been previously reported after hydrogel inlay implantation in corneas, and it has been attributed to the implant's thickness, mechanical factors, and glucose diffusion.[13,74,75] The pathophysiologic significance of epithelial thinning after hydrogel inlays is uncertain and does not seem to affect optical results or intrastromal inlay retention rates.[76]

The absence of changes in endothelial cells shown on histological analysis are consistent with IVCM results evidencing no qualitative or quantitative significant alterations of the endothelium between groups in the GLM repeated measures procedure. Results from both histology and IVCM confirm that

changes related to intrastromal PEGDA implants only affect the stroma and epithelium above the implant, with no evidence of posterior stromal or endothelial changes.

Only one case of biomicroscopically visible haze was described in corneas of group 1, whereas the rest of the corneas remained clear. However, histologic corneal scarring secondary to lamellar dissection was observed in four corneas of group 1. This stromal scarring was consistent with the hyperreflective area represented by a midstromal peak observed on the z-scan graphic by IVCM in corneas of group 1. The stromal structure surrounding implants was similar to previous descriptions after hydrogel inlays of different materials in rabbit and human corneas.[16,21,22,53,55] However, the presence of keratocyte nuclei lining the empty space could indicate the start of a wound healing response caused by fibroblastic transformation of keratocytes that could eventually lead to stromal fibrosis and haze, as has been observed with other implants aimed for refractive purpose, such as the Raindrop inlay. PEGDA inlays were not visible in their original place and shape in contact with the stroma, and the inlay-stromal interface could not be adequately analyzed. It has been reported that high water content and the environmental sensitivity of hydrogels make them unable to be successfully processed for histology by using ordinary tissue-processing techniques, leading to structural changes in the hydrogel-stromal architecture.[53,77,78] Histological processing techniques using a glycol methacrylate-embedding protocol could have avoided expanding and shrinking of the hydrogel as a response to an increase in the pH and could have preserved the structure and morphology of the PEGDA hydrogel intracorneal inlays, as has been described for different types of hydrogels implanted in rabbit corneas.[53,77,78]

Keratocyte nuclei on the edge of lamellar channels were observed in samples of group 2. Cells were arranged in different patterns from nonhomogeneous formations to organized layers of plane cells surrounding the channel.[44,53,55] The presence of keratocyte nuclei on the channels could be attributed to the incapability of the keratocytes to invade PEGDA hydrogel implants and to the intention to fill the potential space generated by the vertical edge of the implants.[44] We did not find lipid deposits, as has been described previously after hydrogel and impermeable intrastromal inlays and ring segment implantation in humans and monkeys.[11,57,79,80] No inflammatory cells were seen except for two cases of eosinophilic infiltration (one in each group). The presence of eosinophils after intrastromal inlay implantations has been reported, although no explanation has been suggested for their presence.[9] The eosinophilic infiltrates in our series corresponded to cases with severe inflammation and infiltration and suggest immunologic origin.

The limitations of this study have been considered. Corneal pockets were performed using a manual technique, and the use of a femtosecond laser could help deliver more regular pocket or flap dissections for the implants, as it has been described for implants aimed at correcting presbyopia.[39] Follow-up time of the study was limited to 2 months. Other studies with a longer duration have shown a higher incidence of complications with hydrogel intrastromal inlays, such as those seen with the Raindrop inlays aimed for refractive purpose, that could arise months or years after intrastromal implantation of synthetic materials.[44,52]

Conclusions

Photopolymerized PEGDA inlays have shown relatively good safety and stability to be used as corneal inlays with therapeutic purpose in rabbit corneas. PEGDA inlays were biostable in the corneal environment and remained clear during follow-up. No significant changes were observed by IVCM in the keratocyte density (anterior and posterior to the implant) nor in the endothelial cell morphology and density. These results were later confirmed by histology. Follow-up time was limited to 2 months, and further studies are required to assess the long-term in vivo biocompatibility with PEGDA inlays for therapeutic purpose.

Acknowledgments

Supported in part by the Spanish Ministry of Science and Education through Apply Research, grant MAT2006-13708-CO2-01. The authors alone are responsible for the content and writing of the paper.

Disclosure: **A. Bidaguren**, None; **J. Mendicute**, None; **I. Madarieta**, Tecnalia (E); **N. Garagorri**, Tecnalia (E)

References

1. Barraquer JI. Queratoplastia refractiva, estudios e informaciones. *Oftalmologicas*. 1949;2:10–30.

2. Barraquer JI. Modification of refraction by means of intracorneal inclusions. *Int Ophthalmol Clin*. 1966;6:53–78.
3. Troutman RC, Swinger C. Refractive keratoplasty: keratophakia and keratomileusis. *Trans Am Ophthalmol Soc*. 1978;76:329–339.
4. Binder PS, Lin L, van de Pol C. Intracorneal inlays for the correction of ametropias. *Eye Contact Lens*. 2015;41:197–203.
5. Choyce DP. The correction of refractive errors with polysulfone corneal inlays; a new frontier to be explored? *Trans Ophthalmol Soc UK*. 1985;104: 332–342.
6. Kirkness CM, Steele AD, Garner A. Polysulphone corneal inlays. Adverse reactions: a preliminary report. *Trans Ophthalmol Soc UK*. 1985; 104:343–350.
7. Lane SL, Lindstrom RL, Cameron JD, et al. Polysulphone corneal lenses. *J Cataract Refract Surg*. 1986;12:50–60.
8. Climenhaga H, MacDonald JM, McCarey BE, Waring GO. Effect of diameter and depth on the response to solid polysulphone intracorneal lenses in cats. *Arch Ophthalmol*. 1988;106:818–824.
9. Deg JK, Binder PS. Histopathology and clinical behavior of polysulphone intracorneal implants in the baboom model. Polysulhone lens implants. *Ophthalmology*. 1988;95:506–515.
10. McCarey BE, Lane SL, Lindstrom RL. Alloplastic corneal lenses. *Int Ophthalmol Clin*. 1988; 28:155–163.
11. Rodrigues MM, McCarey BE, Waring GO, Hidayat AA, Kruth H. Lipid deposits posterior to impermeable intracorneal lenses in rhesus monkeys: clinical, histochemical and ultrastructural studies. *Refract Corneal Surg*. 1990;6:32–37.
12. Horgan SE, Fraser SG, Choyce DP, Alexander WL. Twelve-year follow-up of unfenestrated polysulfone intracorneal lensesin human sighted eyes. *J Cataract Refract Surg*. 1996;22:1045–1051.
13. McCarey BE, Schmidt FH. Modeling glucose distribution in the cornea. *Curr Eye Res*. 1990;9: 1025–1039.
14. Knowles. Effect of intralamellar plastic membranes on corneal physiology. *Am J Ophthalmol*. 1961;51:1146–1156.
15. Dohlman CH, Refojo MF, Rose J. Synthetic polymers in corneal surgery: I. Glyceryl Methacrylate. *Arch Ophthalmol*. 1967;77:252–257.
16. McCarey BE, Andrews DM. Refractive keratoplasty with intrastromal hydrogel lenticular implants. *Invest Ophthalmol Vis Sci*. 1981;21:107–115.
17. Binder PS, Deg JK, Zavala EY, Grossman KR. Hydrogel keratophakia in non-human primates. *Curr Eye Res*. 1981–1982;1:535–542.
18. McCarey BE, Van Rij G, Beekhius WH, Waring GO. Hydrogel keratophakia: a freehand pocket dissection in the monkey model. *Br J Ophthalmol*. 1886;70:187–191.
19. Koenig SB, Hamano T, Yamaguchi T, Kimura T, McDonald MD, Kaufman HE. Refractive keratoplasty with hydrogel implants in monkeys. *Ophthalmic Surg*. 1984;15:225–229.
20. Beekhius W, McCarey BE, Van Rij G, Waring GO. Hydrogel keratophakia: a microkeratome dissection in the monkey model. *Br J Ophthalmol*. 1886;70:192–198.
21. McDonald MB, McCarey BE, Storie B, et al. Assessment of the long-term corneal response to hydrogel intrastromal lenses implanted in monkey eyes for up to five years. *J Cataratct Refr Surg*. 1993;19:213–222.
22. Ismail MM. Correction of hyperopia by intracorneal implants. *J Cataract Refr Surg*. 2002;28: 527–530.
23. Michieletto P, Ligabue E, Balestrazzi A, Balestrazzi A, Giglio S. PermaVision intracorneal lens for the correction of hyperopia. *J Cataract Refract Surg*. 2004;30:2152–2157.
24. Alió JL, Mulet ME, Zapata LF, Vidal MT, De Rojas V, Javaloy J. Intracorneal inlay complicated by intrastromal epithelial opacification. *Arch Ophthalmol*. 2004;122:1441–1446.
25. Güell JL, Velasco F, Guerrero E, Gris O, Pujol J. Confocal microscopy of corneas with an intracorneal lens for hyperopia. *J Refract Surg*. 2004; 20:778–782.
26. Ismail MM. Correction of hyperopia by intracorneal lenses. *J Cataract Refr Surg*. 2006;32: 1657–1660.
27. Verity SM, McCulley JP, Bowman RW, Cavanagh HD, Petroll WM. Outcomes of PermaVision intracorneal implants for the correction of hyperopia. *Am J Ophthalmol*. 2009;147:973–977.
28. Mullet ME, Alió JL, Knorz MC. Hydrogel intracorneal inlays for the correction of hyperopia. Outcomes and complications after 5 years of follow-up. *Ophthalmology*. 2009;116:1455–1460.
29. Saelens IEY, Bleyen I, Hillenaar T, et al. Long–term follow-up of hydrogel intracorneal lenses in two aphakic eyes. *J Cataract Refract Surg*. 2010; 36:2200–2203.
30. Lindstrom RL, MacRae SM, Pepose JY, Hoopes PC. Corneal inlays for presbyopia correction. *Curr Opin Ophthalmol*. 2013;24:281–287.

31. Seyeddain O, Riha W, Hohensinn M, Nix G, Dexl AK, Grabner G. Refractive surgical correction of presbyopia with the AcuFocus small aperture corneal inlay: two-year follow-up. *J Refr Surg*. 2010;26:707–715.
32. Dexl AK, Seyeddain O, Riha W, et al. Reading performance after implantation of a modified corneal inlay design for the surgical correction of presbyopia: 1-year follow-up. *Am J Ophthalmol*. 2012;153:994–1001.
33. Tomita M, Kanamori T, Waring GO IV, et al. Simultaneous corneal inlayimplantation and laser in situ keratomileusis for presbyopia in patients with hyperopia, myopia, or emmetropia: six-month results. *J Cataract Refract Surg*. 2012;38:495–506.
34. Seyeddain O, Hohensinn M, Riha W, et al. Small-aperture corneal inlay for the correction of presbyopia: 3-year follow-up. *J Cataract Refract Surg*. 2012;38:35–45.
35. Dexl AK, Jell G, Strohmaier C, et al. Long-term outcomes after monocular corneal inlay implantation for the surgical compensation of presbyopia. *J Cataract Refract Surg*. 2015;41:566–575.
36. Bouzoukis DI, Kymionis GD, Panagopoulou SI, et al. Visual outcomes and safety of small diameter intrastromal refractive inlay for the corneal compensation of presbyopia. *J Refract Surg*. 2012;28:168–173.
37. Baily C, Kohnen T, O'Keefe M. Preloaded refractive-addition corneal inlay to compensate for presbyopia implanted using a femtosecond laser: one-year visual outcomes and safety. *J Cataract Refract Surg*. 2014;40:1341–1348.
38. Limnopoulou AN, Bouzoukis DI, Kymionis GD, et al. Visual outcomes and safety of a refractive corneal inlay for presbyopia using femtosecond laser. *J Refract Surg*. 2013;29:12–18.
39. Malandrini A, Martone G, Canovetti A, et al. Morphologic study of the cornea by in vivo confocal microscopy and optical coherence tomography after bifocal refractive corneal inlay implantation. *J Cataract Refract Surg*. 2014;40:545–557.
40. Garza EB, Gomez S, Chayet A, Dishler J. One-year safety and efficacy results of a hydrogel inlay to improve near vision in patients with emmetropic presbyopia. *J Refract Surg*. 2013;29:166–172.
41. Whitman J, Dougherty PJ, Parkhurst GD, et al. Treatment of presbyopia in emmetropes using a shape-changing corneal inlay: one-year clinical outcomes. *Ophthalmology*. 2016;123:466–475.
42. Whang WJ, Yoo YS, Joo CK, Yoon G. Changes in keratometric values and corneal high order aberrations after hydrogel inlay implantation. *Am J Ophthalmol*. 2017;173:98–105.
43. Cruise GM, Scharp DS, Hubbell JA. Characterization of permeability and network structure of interfacially photopolymerized poly(ethylene glycol) diacrylate hydrogels. *Biomaterials*. 1998;19:1287–1294.
44. Zheng LL, Vanchinathan V, Dalal R, et al. Biocompatibility of poly(ethylene glycol) and poly(acrylic acid) interpenetrating network hydrogel by intrastromal implantation in rabbit cornea. *J Biomed Mater Res A*. 2015;103:3157–3165.
45. Lee KY, Mooney DJ. Hydrogels for tissue engineering. *Chem Rev*. 2001;101:1869–1879.
46. Myung D, Duhamel P-E, Cochran JR, Noolandi J, Ta CN, Frank CW. Development of hydrogel-based keratoprostheses: a materials perspective. *Biotechnol Prog*. 2008;24:735–741.
47. Bryant SJ, Anseth KS, Lee DA, Bader DL. Crosslinking density influences the morphology of chondrocytes photoencapsulated in PEG hydrogels during the application of compressive strain. *J Orthop Res*. 2004;22:1143–1149.
48. Chirila TV. An overview of the development of artificial corneas with porous skirts and the use of PHEMA for such an application. *Biomaterials*. 2001;22:3311–3117.
49. Nguyen KT, West JL. Photopolymerizable hydrogels for tissue engineering applications. *Biomaterials*. 2002;23:4307–4314.
50. Qiu Y, Park K. Environment-sensitive hydrogels for drug delivery. *Adv Drug Deliv Rev*. 2001;53:321–339.
51. Xie RZ, Evans MD, Bojarski B, et al. Two-year preclinical testing of perfluoropolyether polymer as a corneal inlay. *Invest Ophthalmol Vis Sci*. 2006;47:574–581.
52. Farooqui N, Myung D, Koh W, et al. Histological processing of pH-sensitive hydrogels used in corneal implant applications. *J Histotechnol*. 2007;30:157–163.
53. Tan XW, Hartman L, Tan KP, et al. In vivo biocompatibility of two PEG/PAA interpenetrating polymer networks as corneal inlays following deep stromal pocket implantation. *J Mater Sci Mater Med*. 2013;24:967–977.
54. Salamatrad A, Jabbarvand M, Hashemian H, Khodaparast M, Askarizadeh F. Histological and confocal changes in rabbit cornea produced by an intrastromal inlay made of hexafocon A. *Cornea*. 2015;34:78–81.
55. Hartmann L, Watanabe K, Zheng LL, et al. Toward the development of an artificial cornea: improved stability of interpenetrating polymer

networks. *J Biomed Mater Res B Appl Biomater*. 2011;98:8–17.
56. Garagorri N, Fermanian S, Thibault R, et al. Keratocyte behavior in three-dimensional photopolymerizable poly(ethylene glycol) hydrogels. *Acta Biomater*. 2008;4:1139–4117.
57. Parks RA, McCarey BE, Knight PM, Storie BR. Intrastromal crystalline deposits following hydrogel keratophakia in monkeys. *Cornea*. 1993;12: 29–34.
58. Beekhius WH, McCarey BE, van Rij G, Waring GO III. Complications of hydrogel intracorneal lenses in monkeys. *Arch Ophthalmol*. 1987;105: 116–122.
59. Robin JB, Regis-Pacheco LF, Kash RL, Schanzlin DJ. The histopathology of corneal neovascularization. inhibitor effects. *Arch Ophthalmol*. 1985;103:284–287.
60. Phillips K, Arffa R, Cintron C, et al. Effects of prednisolone and medroxyprogesteroneon corneal wound healing, ulceration, and neovascularization. *Arch Ophthalmol*. 1983;101:640–643.
61. Hicks CR, Crawford GJ. Melting after keratoprosthesis implantation: the effects of medroxyprogesterone. *Cornea*. 2003;22:497–500.
62. Abdelkader A, Elewah el-SM, Kaufman HE. Confocal microscopy of corneal wound healing after deep lamellar keratoplasty in rabbits. *Arch Ophthalmol*. 2010;128:75–80.
63. Mohan RR, Hutcheon AE, Choi R, et al. Apoptosis, necrosis, proliferation, and myofibroblast generation in the stroma following LASIK and PRK. *Exp Eye Res*. 2003;76:71–87.
64. Petroll WM, Boettcher K, Barry P, Cavanagh HD, Jester JV. Quantitative assessment of anteroposterior keratocyte density in the normal rabbit cornea. *Cornea*. 1995;14:3–9.
65. Twa MD, Giese MJ. Assessment of corneal thickness and keratocyte density in a rabbit model of laser in situ keratomileusis using scanning laser confocal microscopy. *Am J Ophthalmol*. 2011;152:941–953.
66. Erie JC, Patel SV, McLaren JW, Hodge DO, Bourne WM. Corneal keratocyte deficits after photorefractive keratectomy and laser in situ keratomileusis. *Am J Ophthalmol*. 2006;141:799–809.
67. Pisella PJ, Auzerie O, Bokobza Y, Debbasch C, Baudouin C. Evaluation of corneal stromal changes in vivo after laser in situ keratomileusis with confocal microscopy. *Ophthalmology*. 2001; 108:1744–1750.
68. Ali Javadi M, Kanavi MR, Mahdavi M, et al. Comparison of keratocyte density between keratoconus, post-laser in situ keratomileusis keratectasia, and uncomplicated post-laser in situ keratomileusis cases. A confocal scan study. *Cornea*. 2009;28:774–779.
69. Mitooka K, Ramirez M, Maguire LJ, et al. Keratocyte density of central human cornea after laser in situ keratomileusis. *Am J Ophthalmol*. 2002;133:307–314.
70. Perez-Gomez I, Efron N. Change to corneal morphology after refractive surgery (myopic laser in situ keratomileusis) as viewed with a confocal microscope. *Optom Vis Sci*. 2003;80:690–697.
71. Müller LJ, Marfurt CF, Kruse F, Tervo TM. Corneal nerves: structure, contents and function. *Exp Eye Res*. 2003;76:521–542.
72. Erie JC, Patel SV, McLaren JW, et al. Effect of myopic laser in situ keratomileusis on epithelial and stromal thickness: a confocal microscopy study. *Ophthalmology*. 2002;109:1447–1452.
73. Kato T, Nakayasu K, Hosoda Y, Watanabe Y, Kanai A. Corneal wound healing following laser in situ keratomileusis (LASIK): a histopathological study in rabbits. *Br J Ophthalmol*. 1999;83: 1302–1305.
74. Samples JR, Binder PS, Zavala EY, Baumgartner SD, Deg JK. Morphology of hydrogel implants used for refractive keratoplasty. *Invest Ophthalmol Vis Sci*. 1984;25:843–850.
75. McCarey BE, Andrews DM, Hatchell DL, Pederson H. Hydrogel implants for refractive keratoplasty: corneal morphology. *Curr Eye Res*. 1982;2:29–38.
76. Crawford GJ, Chirila TV, Vijayasekaran S, Dalton PD, Constable J. Preliminary evaluation of a hydrogel core-and-skirt keratoprosthesis in the rabbit cornea. *J Refract Surg*. 1996;12:125–129.
77. James R, Jenkins L, Ellis SE, Burg KJL. Histological processing of hydrogel scaffolds for tissue-engineering applications. *J Histotechnol*. 2004;27:133–139.
78. Webster SS, Jenkins L, Burg KJL. Histological techniques for porous, absorbable, polymeric scaffolds used in tissue engineering. *J Histotechnol*. 2003;26:57–65.
79. Spirn MJ, Dawson DG, Rubinfeld RS, et al. Histopathological analysis of post-laser-assisted in situ keratomileusis corneal ectasia with intrastromal corneal ring segments. *Arch Ophthalmol*. 2005;123:1604–1607.
80. Roth SI, Stock EL, Siel JM, et al. Pathogenesis of experimental lipid keratopathy. An ultrastructural study of an animal model system. *Invest Ophthalmol Vis Sci*. 1988;29:1544–1551.